Concentrated winding machines fed by PWM inverters: insulation design helped by simulations based on equivalent circuits

Daniel Roger, Mustapha Toudji, Stéphane Duchesne, Guillaume Parent

Concentrated winding machines fed by PWM inverters: insulation design helped by simulations based on equivalent circuits

Daniel Roger, Mustapha Toudji, Stéphane Duchesne, Guillaume Parent
Univ. Artois - EA4025, LSEE, 62400 Bethune – FRANCE
daniel.roger@univ-artois.fr

Abstract* - *In more electric aircrafts, the fast-fronted pulses imposed by PWM inverters to the motor windings may cause an earlier aging of the thin polymer layers of the electrical insulation system (EIS). In low-pressure environments, the voltage distribution in all the components of the EIS is major issue for designing long-life electrical machines. The voltage stresses in the thin insulating layers of the compact machines must remain under control for avoiding partial discharges (PD). The paper proposes an approach based on High Frequency (HF) equivalent circuits for analyzing the resonances in a motor winding. The paper focuses on the windings of permanent magnet synchronous machines built with one coil per stator slot.

I. INTRODUCTION

Electrical machines are used for many applications; they can produce high torques with an accurate control of the mechanical loads when high-performance power electronic converters feed them. The permanent magnet synchronous machine (PSMS) is the best solution for producing high torques in small volumes. However, the fast-fronted voltage pulses imposed by the inverter cause voltage spikes in the windings during the electrical transients following each fast-fronted voltage step. The damages caused by this electrical stress are more severe when the machine is used in aircrafts because the partial discharge inception voltage (PDIV) is lower at low air pressures. PDs may appear and shorten the EIS live span [1]. Therefore, the prediction of short voltage spikes in windings is a major issue [2, 3].

For the standard distributed windings, the wires of each coil are placed in stator slots for obtaining a spatial distribution along the air gap close to an ideal sine wave. For small machines made with round enameled wires, the exact relative position of each turn in a slot is unknown. The winding is not deterministic; it has random properties. The probability to have the input turn adjacent to the output one cannot be neglected [4]. For this case, the full coil voltage is imposed to the turn-to-turn insulation made of two thin polymer layers and cause PD. Consequently, the distributed winding machines cannot be used in low-pressure environments without additional filter able to soften the fronts of the voltage pulses. The mass of such a filter is a big drawback in aeronautics.

The concentrated winding technology is a good solution because the motor is built with one prefabricated coil per tooth. The simple-shaped coils are wound by automatic machines that place each turn at a known relative position; the winding is deterministic. With deterministic coils, the voltage distribution between turns inside coils and between coils can be computed during the transients that follow each fast-fronted voltage step.

More over, the concentrated windings permanent magnet synchronous machines (CW-PMSM) have shorter end-winding connections; copper losses are lower. The main drawback of this technology is a higher cogging torque, but it remains acceptable when specific rules are observed for the number of rotor poles and of stator slots [5].

The paper proposes an approach based on high frequency (HF) equivalent circuits for analyzing the short transients in the windings of a CW-PSMS and the corresponding distribution of voltage spikes. The proposed approach is based on several simplifications that are detailed and discussed on the basis of impedance spectra.

II. EQUIVALENR CIRCUIT CONSTRUCTION AND SIMPLIFYING HYPOTHESES

A. CW-PMSM winding description

Explanations are made considering a wide spread CW-PSMS made with a 24-slot stator and a 18-pole rotor fed by a 3-phase inverter. Fig. 1 presents the connections of the 8 coils of the Phase A. The other phases are similar. These connections produce a 18-pole rotating field that interacts with the 18-pole rotor for producing a non-zero mean torque. This interaction produces also limited cogging torques.

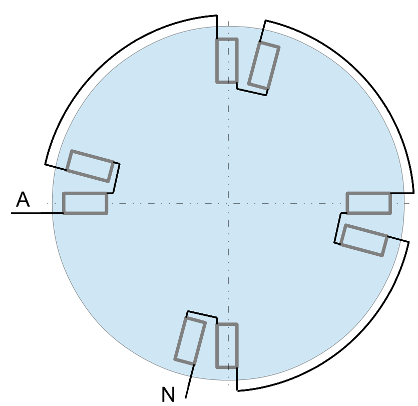

Fig. 1. Phase A of a 18 poles 24 teeth CW-PSMS made of 4 coil-pairs.

For the high-speed machine of the example, the 24 coils are made of 14 turns wound on two layers as shown in Fig. 2. The enameled wire is a standard PEI-PAI product, the copper diameter is *0.85mm* and the polymer layer thickness is $45\mu m$. A *100μm* thick polymer sheet reinforces the insulation between the layers. The ground insulation is made by another polymer sheet of 200μm. The magnetic core length is *50mm*. With these sizes the length of a turn in the inner coil is *126mm* and, considering the center of the wire, the cross section for the magnetic flux is $472mm^2$ for the first layer and $556mm^2$ for the outer one.

The HF study is performed for a phase alone, neglecting the probability of having a voltage steep imposed simultaneously on two phases at the microsecond time-scale. Considering classical PWM algorithms and switching frequencies on the one hand and the rise time of standard IGBTs and the following transients duration on the other hand, the probability of having an interaction of two commutations on different phases is under 1%. Therefore, for the HF transients can be studied on a phase alone, considering that the other ones are in steady states.

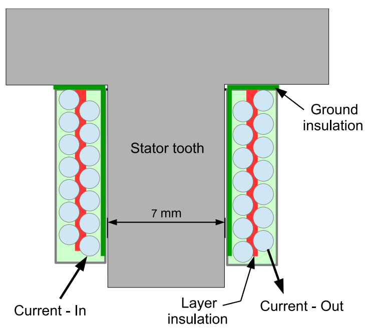

Fig. 2. Stator tooth and the two-layer coil. The magnetic core length is 50mm.

B. *Influence of the magnetic stator core at high frequencies*

The magnetic core is made of high-performance magnetic FeCo sheets [6] wide spread for building high performance motors. The magnetic sheet thickness is $0.35m$; the saturation shoulder is at *2.35T*; the electric resistivity is $\rho = 40\,10^{-8}\,\Omega.m$. Magnetic sheets have non-linear characteristics; the relative permeability depends on the operating point. For this material, the maximum value is $\mu_{Rmax} \approx 13000$. At a given time, the relative permeability of the magnetic material that must be considered for studying HF small signals is not the same for every stator teeth because the magnetic operating point is imposed by the rotor position.

For high frequencies, in the range of the natural frequencies of the transients excited by the fast-fronted voltage steps, the penetration depth of the magnetic field under each side of the sheets is very small. For instance, at $f = 1MHz$ and for the maximum relative permeability, the skin depth is:

$$\delta = \sqrt{\frac{\rho}{\pi\mu_0\mu_R f}} = 2.8\mu m \tag{1}$$

The field penetration corresponds to 0.75% of the sheet thickness on each side. Only 1.5% of the sheet is used: the iron core has a low influence on the coil HF inductances. However, eddy-currents inside the skin depth of each sheet create losses that can be modeled as additional resistances in the HF equivalent circuit.

Noting z the axis of the motor, which is perpendicular to the magnetic surface of each sheet, the penetration of the magnetic field in a sheet is given by the equation of a damped wave in a conducting media described by (2). In this expression H_0 is the magnetic field, parallel to the sheet surface, imposed at its border by the HF current in the coil. Expression (2) is obtained by a 1D analysis along the z-axis penetrating inside a sheet from the point z=0 that corresponds to the sheet surface. The analysis supposes also that the sheet thickness is much larger than the skin depth δ.

$$H(z,t) = H_O \exp\left(-\frac{z}{\delta}\right)\cos\left(\omega t - \frac{z}{\delta}\right) \tag{2}$$

In 1D, the current density of eddy currents $J(z,t)$ can be computed from (2) by a derivation relative to the space variable z.

$$J(z,t) = -\frac{dH(z,t)}{dz} \tag{3}$$

$$J(z,t) = H_O\frac{\sqrt{2}}{\delta}\exp\left(\frac{-z}{\delta}\right)\cos\left(\omega t - \frac{z}{\delta} + \frac{\pi}{4}\right) \tag{4}$$

The instantaneous power density $p_v(z,t)$, expressed in W/m^3, at any point inside the magnetic sheet depends on the square of the current density and on the metal resistivity:

$$p_v(z,t) = \rho J^2 \tag{5}$$

This instantaneous power density is used for determining the average power density at any point z inside the sheet:

$$P_v(z) = \rho\frac{H_0^2}{\delta^2}\exp\left(\frac{-2z}{\delta}\right) \tag{6}$$

Considering that the sheet thickness is much larger than the skin depth, the average power under any point of the sheet surface, expressed in W/m^2, is obtained by integrating the volume power density along the z-axis.

$$P_s = \int_{z=0}^{z\to\infty}\rho\frac{H_0^2}{\delta^2}\exp\left(\frac{-2z}{\delta}\right)dz = \frac{\rho}{2\delta}H_0^2 \tag{7}$$

The last step consist in estimating the magnetic field H_0 at any point of the surface of the magnetic sheets excited by the HF current in coils. Fig. 3 presents details on the magnetic core around a set of two consecutive coils of a CW-PMSM, where field lines are roughly drawn. The length of a field line l_F can be estimated considering the stator geometry.

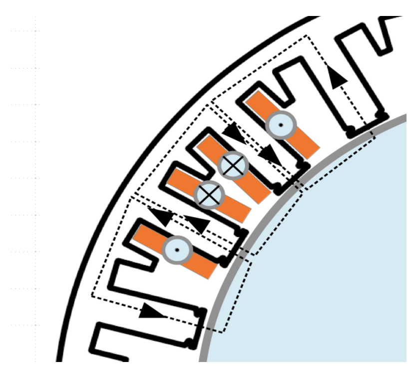

Fig. 3. Magnetic core around two consecutive coils of a CW-PMSM.

In Fig. 3, the direction each field line corresponds to the series connection imposed by the CW-PMSM winding structure. The magnetic field created by the HF current component I_{0RMS} in the N turn of a coil can be estimated roughly considering the elementary field H_1 defined in (8).

$$H_1 \approx \frac{N I_{0RMS}\sqrt{2}}{l_F} \tag{8}$$

Fig. 3 shows that, for a set of two consecutive coils, 4 teeth must be considered, the two central teeth are excited by $2H_1$ and the lateral ones by H_1 as the slot back and the rotor surface. For a laminated stator made of N_L sheets, HF iron losses P_I in the part of the stator corresponding to a single coil can be computed from (9) that considers the surface of a tooth S_T and the surface of a slot back S_B when the HF losses in the rotor are neglected.

$$P_I \approx 2N_L\left[\frac{\rho}{2\delta}\,(2H_1)^2\,S_T + \frac{\rho}{2\delta}\,(H_1)^2(2S_B + S_T)\right] \tag{9}$$

or

$$P_I \approx N_L\frac{\rho}{\delta}\,H_1^2(5\,S_T + 2S_B) \tag{10}$$

From (10), and replacing H_1 by its value defined in (8), it is possible to consider the current I_{0RMS} flowing in an equivalent resistance R_{eq} per turn that produces the same iron losses.

$$R_{eq}I_{0RMS}^2 \approx N_L\frac{\rho}{\delta}\left[\frac{N I_{0RMS}\sqrt{2}}{l_F}\right]^2(5\,S_T + 2S_B) \tag{10}$$

The expression of the equivalent resistance connected in series with the 2 coils of Fig. 3 appears after simplifying (10)

$$R_{eq} \approx 2N_L\frac{\rho}{\delta}\frac{N^2}{l_F^2}\,(5\,S_T + 2S_B) \tag{11}$$

For exploiting this equivalent resistance in the HF equivalent circuit made at the turn level, we must remind that the power has been computed for 2 consecutive coils of N turns each.

$$R_{eq1} = \frac{R_{eq}}{2N} \approx N_L\frac{\rho}{\delta}\frac{N}{l_F^2}\,(5\,S_T + 2S_B) \tag{12}$$

For the example of CW-PMSM, the parameters are: N_L=143; $L_F \approx 70mm$; $S_B \approx 115mm^2$; $S_T \approx 112mm^2$. Fig. 4 shows the variations of this equivalent resistance per turn, from 100kHz to 10MHz and for two values of the iron core relative permeability.

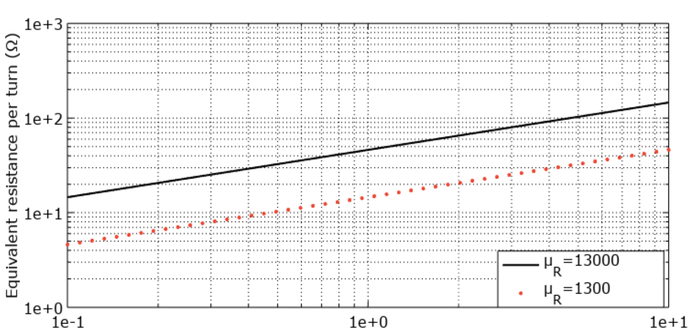

Fig. 4. Equivalent resistance per turn representing the eddy current losses in the CW-PMSM laminated core for a coil-pair.

C. HF Equivalent circuit of a layer

Each layer is modeled by a RLC equivalent circuit built at the turn level. Fig. 5 shows the 8 nodes of a 7-turn layer following a method previously defined [7]. Each turn has a resistance corresponding to the copper and iron losses at the considered frequency, a self-inductance and a magnetic coupling with the other turns, which corresponds to 6+5+4+3+2+1=21 mutual inductances. The 6 turn-to-turn capacitances are added at the turn level, they are connected between the nodes corresponding to the ends of turns. The other capacitances are considered when the layers are assembled for forming a coil.

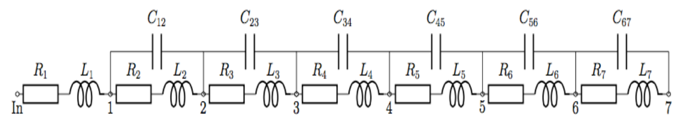

Fig. 5. Equivalent circuit of a 7-turn layer of a coil.

Two 2D FEM simulations that consider the geometry of a single-layer 7-turn coil in air determine the parameters. The first one is performed in DC with the electrostatic equations and a mesh able to compute the electric field in the insulation layers yields the turn-to-turn capacitances. Results are: C_{12}=9.6pF; C_{23}=9.3pF; C_{34}=9.3pF; C_{45}=9.3pF; C_{56}=9.3pF; C_{67}=9.6pF. Capacitances computed between non-adjacent turns, which are one hundred times lower, are neglected.

The second FEM simulation, made with a sine excitation at several frequencies, computes the magnetic self and mutual inductances, considering the skin and proximity effects in the copper wires and a 7-turn layer in air. Table 1 shows a part of the parameters for the inner layer. It shows that, despite the very strong skin and proximity effects in the copper wire, the inductances stays in the same range of values.

TABLE I. Self inductances and a part of the 21 mutual inductances of a single layer 7-turn coil in air.

	50 Hz (no HF effects)	500 MHz (very Strong HF effects)
L_1	35.6 nH	27.3 nH
L_2	35.7 nH	25.6 nH
M_{12}	22.8 nH	20.3 nH
M_{13}	14.9 nH	15.7 nH
M_{14}	10.6 nH	12.4 nH
M_{15}	7.7 nH	10.0 nH
M_{16}	5.8 nH	8.3 nH
M_{17}	4.4 nH	7.0 nH

The skin and proximity effects in the copper wire have also an influence on the copper resistance but the resistances obtained for a turn by the FEM simulation of the coil in air remains are much lower than the equivalent resistance per turn due to the skin effects in the iron laminated core.

The impedance spectrum of the single-layer 7-turn coil is computed from the equivalent circuit of Fig. 5 considering only the equivalent resistance per turn due to the FeCo laminated core, the self and mutual inductances and the turn-to-turn capacitances. Results are presented in Fig. 6.

It can be seen that the natural parallel (f_P) and series (f_S) frequencies are over 100MHz which is much higher than the usual voltage oscillations frequency observed experimentally on a motor winding fed by fast-fronted pulses. However, the result analysis gives the self inductance for each layer. Results are $L_{eq1} = 762nH$ for the inner layer and $L_{eq2} = 880nH$ for the outer one.

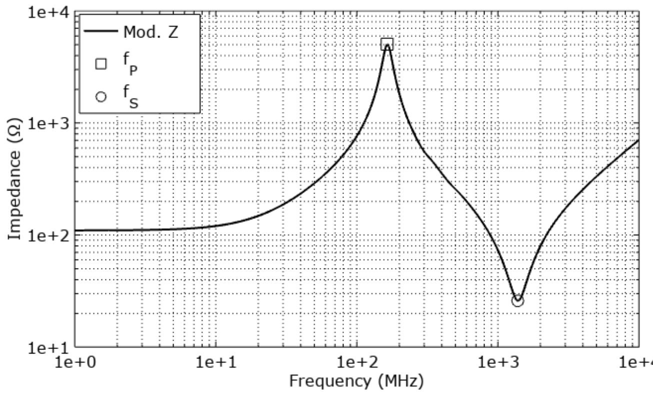

Fig. 6. Spectrum impedance simulated for a 1-layer 7-turn coil.

C. *HF Equivalent circuit of a coil*

A stator coil is made of several layers that can be modeled by a RLC equivalent circuit built at the layer level. The analysis at this level involves the inductances of layers, the magnetic coupling between them, the layer-to-layer capacitances and layer-to-ground ones. Fig. 7 details this idea. Each layer is split in two parts for connecting the capacitances to the nodes situated at their centers. The capacitances estimations are obtained considering equivalent plane capacitances where the electrode surfaces are defines by by the slot and the coil geometries; the thickness of the corresponding insulation sheet gives the and distance between the electrodes. Results are $C_{12} = 410pF$; $C_{1G} = 180pF$ and $C_{2G} = 34pF$. Each half layer has a self and mutual inductances corresponding to the half of the turn number of a full layer.

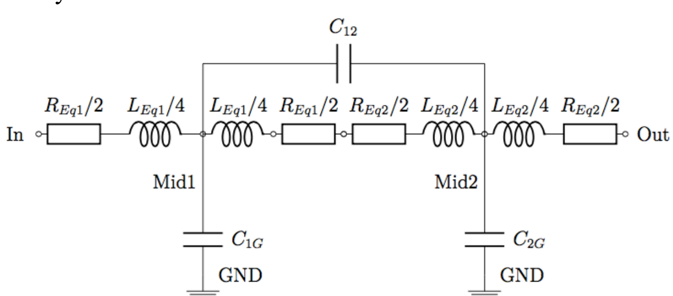

Fig. 7. HF simplified equivalent circuit of a coil.

C. *Experimental elements and discussion*

An impedance spectrum was measured considering 2 coils placed on consecutive slots of the FeCo stator. Fig. 8. Presents the experimental results and the simulation ones. The model consists of twice the equivalent circuit of fig. 7, adding the magnetic couplings defined in fig. 3. The capacitance between the outer surfaces of coils is neglected because of the small surfaces and the relatively long distance in air. The comparison shows that the equivalent circuit predicts a parallel resonance in the correct frequency range but a lower accuracy at higher frequencies: the model must be improved. One of the key parameters is the choice of the connection points of the capacitances in the equivalent circuits. In fact, an equivalent circuit with capacitances is a discrete representation of electric fields in dielectrics, which are distributed phenomena. Another key point is the approximations that suppose the same equivalent resistance for considering the skin effect in the magnetic sheets. In a real motor the stator teeth have not the same magnetic operating point.

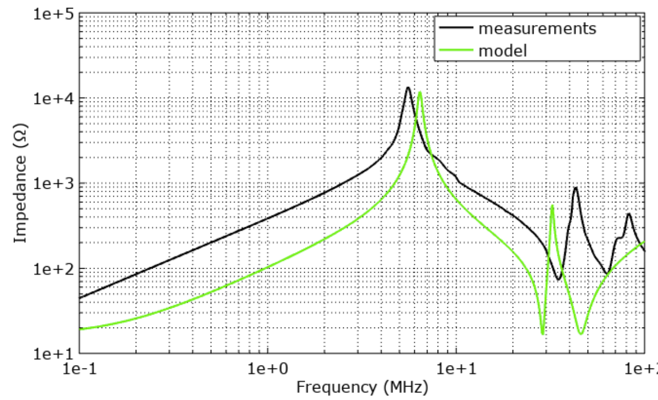

Fig. 8. Impedance spectrum of two consecutive coils connected in series.

CONCLUSION

A method based on HF electric equivalent circuits is proposed for determining the behavior of the machine winding during the short transient states following the fast-fronted voltage steps imposed by PWM inverters. The paper is based on the analysis of a CW-PMSM that has deterministic coils. Simplifications are proposed considering several levels: turn, layer, coil and pair of consecutive coils. This approach yields interesting results with a simple equivalent circuit at each level, but two key points require a deeper study: the influence of the variations of the magnetic core operating point and the generalization of a method for performing the best choice of the nodes where the stray capacitance should be connected for producing the optimal HF equivalent circuit. With such equivalent circuits, it will be possible to compute the voltage spikes everywhere inside the machine winding with a standard circuit simulator using its transient analysis capabilities.

REFERENCES

[1] E. Sili, "Etude et caractérisation des décharges partielles et du vieillissement du polyimide en environnement aéronautique," Ph.D thesis, Laplace, Université Paul Sabatier, Toulouse, Dec. 2012.

[2] S. Islam and G. Ledwich, "An equivalent circuit for calculation of interturn voltage distribution of stator windings in the presence of slot discharges," in *Proc. 5th Int. Conf. Properties Appl. Dielectr. Mater.*, vol. 1. May 1997, pp. 507–510.

[3] F. Perisse, P. Werynski, and D. Roger, "A new method for AC machine turn insulation diagnostic based on high frequency resonances," *IEEE Trans. Dielectr. Electr. Insul.*, vol. 14, no. 5, pp. 1308–1315, Oct. 2007.

[4] S. Duchesne, V. Mihaila, G. Velu and D. Roger, "Study of wire distribution in a slot of a motor fed by steep fronted pulses for lifetime extension," IEEE International Symposium on Electrical Insulation ISEI - San Juan (USA), 2012.

[5] J. Purhonen,T. Jokinen and V. Hrabovcova, "Design of rotating electrical machines," John Wiley and Sons, 2008.

[6] "Soft magnetic materials and semi-finished products," in Vaccum-Schmeze GmbH data sheet, 2002.

[7] M. Toudji and G. Parent and S. Duchesne and P. Dular, "Determination of Winding Lumped Parameter Equivalent Circuit by Means of Finite Element Method," EEE Transactions on Magnetics, vol. 53, No. 6, June 2017, pp. 1-4.